SCIENTIFIC REPORTS

OPEN

SUBJECT AREAS:
MATERIALS FOR ENERGY AND CATALYSIS
MECHANICAL PROPERTIES
MATERIALS SCIENCE
ATOMISTIC MODELS

Received
4 June 2013

Accepted
2 September 2013

Published
26 September 2013

Correspondence and requests for materials should be addressed to S.W. (towangshuai@eng.hokudai.ac.jp)

# Hydrogen-induced change in core structures of {110}[111] edge and {110}[111] screw dislocations in iron

Shuai Wang, Naoyuki Hashimoto & Somei Ohnuki

Lab of Advanced Material, Graduate School of Engineering, Hokkaido University, N-13, W-8, Sapporo 060-8278, Japan.

**Employing the empirical embedded-atom method potentials, the evolution of edge and screw dislocation core structure is calculated at different hydrogen concentrations. With hydrogen, the core energy and Peierls potential are reduced for all dislocations. A broaden-core and a quasi-split core structure are observed for edge and screw dislocation respectively. The screw dislocation and hydrogen interaction in body-centred cubic iron is found to be not mainly due to the change of elastic modulus, but the variation of dislocation core structure.**

Much attention has been paid on the hydrogen and dislocation interactions, which is of importance for understanding the internal mechanism of hydrogen embrittlement problem. However, if we review the past researches, most of the H-dislocation interaction models actually focus on edge dislocation[1] or edge partials of screw dislocation[2]. For instance, in the hydrogen enhanced plasticity model (HELP)[3] that now becomes one of the most accepted theories, the screw-H interaction is ruled out due to a assumption of isotropic strain field for H atoms. This assumption has no problem with FCC metals, as we argued elsewhere[4], due to the anisotropic strain field of H atoms in BCC metals, the short-range screw-H interaction is possible. Many density function theory (DFT) and molecular dynamics (MD) calculations have reported the trapping of hydrogen on the screw core and changes in kink pair nucleation[5–7], but there is a paucity of studies on the hydrogen effect on evolution of dislocation core structure. The screw-H interaction in BCC iron needs to be investigated by simulation and experimental works.

In this report, we will introduce the analysis of dislocation core structures and the Peierls barriers at different hydrogen concentrations by using a DFT based embedded atom method (EAM) potential. The edge-H and screw-H interaction will be discussed based on the simulation results.

## Results

Here we consider an isolated edge dislocation with Burgers vector 1/2[111], slip plane normal $[\bar{1}10]$, and line direction $[\bar{1}12]$. Using the method of Cai[8], we firstly create a perfect crystal satisfying the periodic boundary conditions (PBC) with dimensions 20[111], 20$[\bar{1}10]$, 30$[\bar{1}\bar{1}2]$ along the X, Y, Z axes. Then the 1/4 of the atomic layers normal to the $[\bar{1}10]$direction are removed to create two free surfaces (with two 1/8 vacuum regions). Edge dislocation was introduced as dipole by the linear elasticity solution of atom displacement field. As one of the two dislocations in the dipole is intentionally introduced into the vacuum region, only one dislocation remains after minimization. The edge dislocation system contains 106560 atoms (97.64 Å × 80.75 Å × 209.67 Å). As illustrated in Fig. 1a, the dislocation was detected by using common neighbour analysis[9]. By the similar method, an isolated $1/2\langle 111\rangle\{\bar{1}10\}$ screw dislocation was created, as shown in Fig. 1b. The screw dislocation system contains 108000 atoms (98.87 Å × 80.75 Å × 209.67 Å). The image force produced by these two free surface is given by[10]:

$$F_{img} = \frac{-\mu b^2}{4\pi}\left(\frac{1}{d_1} - \frac{1}{d_2}\right) \tag{1}$$

where $\mu$ is the shear modulus of Fe, $d_1$ and $d_2$ are the distances of the dislocation from the two surfaces. Because the glide planes for the two dislocations are located at the half length of Y axis, the $F_{img}$ in our simulation box is negligible.

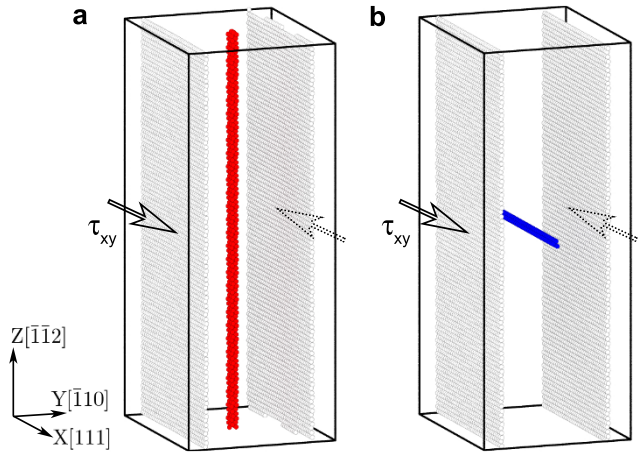


**Figure 1 | Schematic geometric of two types of dislocation used in simulation: (a) 1/2⟨111⟩{1̄10} edge dislocation; (b) 1/2⟨111⟩{1̄10} screw dislocation.**

Peierls energy and evolution of dislocation core structure were analysed at different hydrogen concentrations. Hydrogen atoms were initially putted near to the dislocation core (1*b* distance), and their positions were optimised by the CG method. We will use H atom per dislocation length ($nm^{-1}$) to measure the hydrogen concentration.

The trap energy of hydrogen atom on dislocations can be calculated following the equation[5]

$$E_{trap} = \left[E\left(Fe_0^N, H^n\right) - E\left(Fe_0^N\right)\right] - \left[E\left(Fe_d^N, H^n\right) - E_d^N\right] \qquad (2)$$

where $N$ and $n$ in the right side denote crystals containing $N$ Fe atom and $n$ H atom, $E\left(Fe_0^N\right)$ and $E\left(Fe_0^N, H^n\right)$ are potential energies of a perfect crystal without and with hydrogen, and $E\left(Fe_d^N\right)$ and $E\left(Fe_d^N, H^n\right)$ are potential energies of a dislocation system without and with hydrogen. By using Eq. 2, hydrogen has trap energies of $E_{trap}^{edge} = 0.33$ eV per atom at the assigned position near edge dislocations, and $E_{trap}^{screw} = 0.18$ eV per atom at the assigned position near screw dislocations.

By plotting stress versus strain curve in the NVT shear process, the shear modulus $\mu$ can be obtained by a linear fitting of elastic region, and the stress at time when dislocation moves a large distance is the Peierls stress $\sigma_p$[8]. The energy of a straight dislocation line can be expressed as:

$$E = E_{core} + Kb^3 \ln(R/r_c) \qquad (3)$$

per $b$[10], where $E_{core}$ is the dislocation core energy, $K$ depends on the elastic constants, $R$ is a long-range cutoff, and $r_c$ is a short-range cutoff. We took a $r_c = 2b$ and the $E_{core}$ was obtained by subtract the potential energy of perfect lattice from that of a dislocation-centred cylinder with $R = r_c$. The $\sigma_p$, $\mu$, and $E_{core}$ for dislocation with different hydrogen concentrations are shown in Table 1. The $\sigma_p$ and $E_{core}$ of all dislocations decrease as the number of hydrogen atoms increases. The shear modulus of edge system decreases with the appearance of hydrogen, which indicates that hydrogen can influence the edge dislocation motion via the second order interaction in HELP theory[3]. By contrast, $\mu$ for screw dislocation system is hardly changed. The expected H interaction with screw dislocation according to the second order interaction was not observed[1,2].

Figure 2 shows energy barriers for dislocations moving 1*b* at different hydrogen concentrations. In Fig. 2a, Peierls potential ($E_p$) of hydrogen-free edge dislocation is about 0.7 meV/b. With hydrogen the height of barrier decreases and at $C_H = 0.43$ $E_p$ is only 0.05 meV/b. The hydrogen-free screw dislocation in Fig. 2b has a $E_p$ around 10 meV/b, which is consistent with the calculation using the classical

Table 1 | Peierls stress ($\sigma_p$), Shear modulus ($\mu$) and dislocation core energy ($E_{core}$) at different hydrogen concentrations

| $C_H$ ($nm^{-1}$) | $\sigma_p$ (GPa) | $\mu$ (GPa) | $E_{core}$ (meV/Å) |
|---|---|---|---|
| edge-0 | 0.057 | 74.58 | 395.74 |
| edge-0.05 | 0.045 | 71.48 | 387.90 |
| edge-0.14 | 0.028 | 71.08 | 361.16 |
| edge-0.24 | 0.024 | 65.32 | 332.45 |
| edge-0.33 | 0.019 | 57.37 | 306.91 |
| edge-0.43 | 0.013 | 52.25 | 284.20 |
| screw-0 | 0.90 | 69.93 | 278.59 |
| screw-0.10 | 0.46 | 69.70 | 263.19 |
| screw-0.30 | 0.32 | 69.55 | 210.03 |
| screw-0.51 | 0.30 | 69.47 | 155.21 |
| screw-0.71 | 0.31 | 69.54 | 101.67 |
| screw-0.91 | 0.31 | 70.77 | 10.27 |

EAM potential of Mendelev[11]. Same as the Medelvel's potential, there is a local minimum at the 0.5*b* position. This intermediate metastable configuration, already reported in Refs. 12 and 13, corresponds to the split core described by Takeuchi[14]. The $E_p$ of screw dislocation also

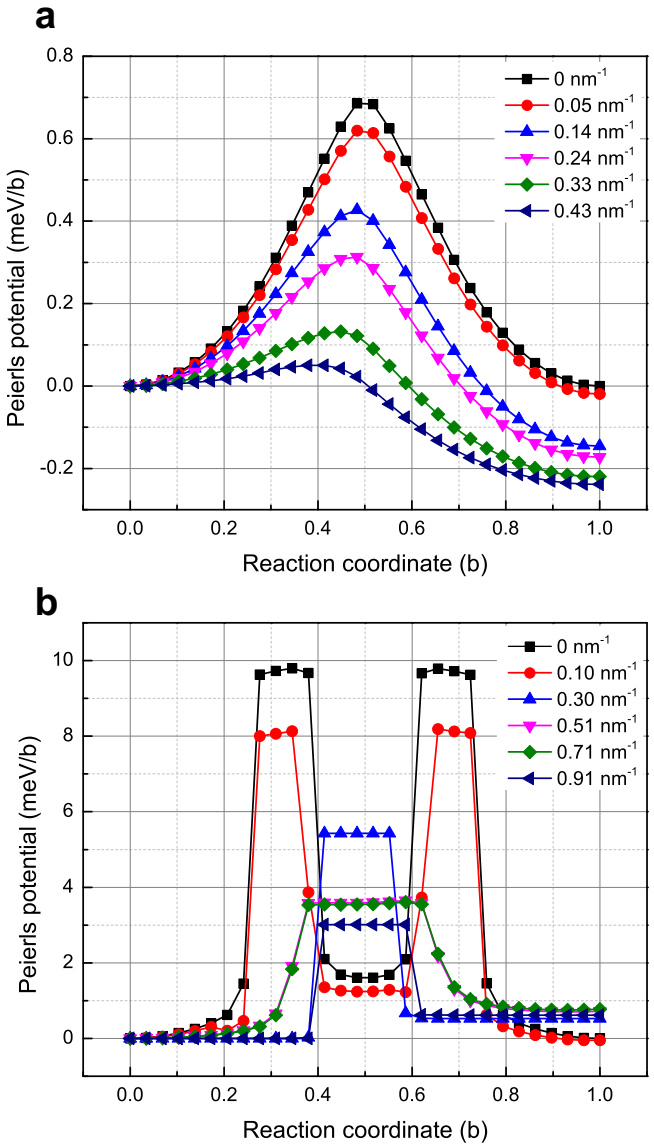


**Figure 2 | Potential energy barriers along MEPs of dislocations with different hydrogen concentrations: (a) edge dislocation; (b) screw dislocation.**

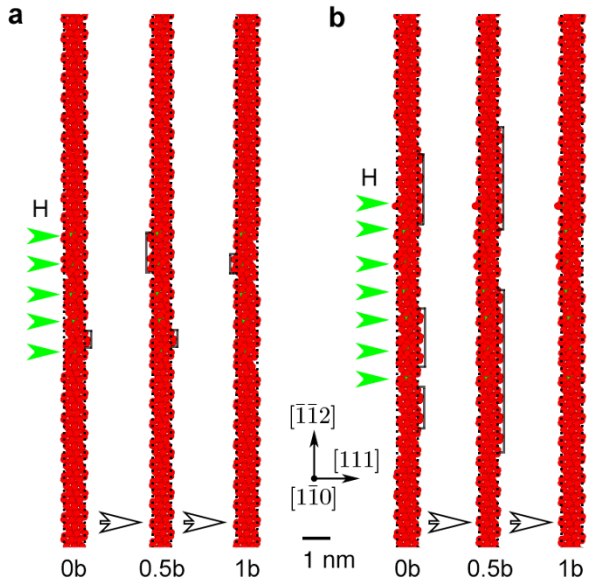


**Figure 3 | The evolution of core structures of edge dislocation at different hydrogen concentrations: (a) at hydrogen concentration of 0.24 nm$^{-1}$; (b) at hydrogen concentration of 0.33 nm$^{-1}$.**

decreases as $C_H$ increases. The camel hump peak changes to a single hump type at $C_H$ higher than 0.30 nm$^{-1}$.

Without hydrogen, the migration of edge dislocation has no formation of kinks or change of core structure. Equilibrated hydrogen positions are under the extra atomic plane of edge dislocation as marked with arrow heads in Fig. 3. With 0.24 nm$^{-1}$ hydrogen (Fig. 3a), a column of atoms propagates towards the [111] direction, with a height of $a[\bar{1}\bar{1}2]$ and a width around $a/2[111]$. In the final image, the atoms propagated to the [111] direction reach the 1$b$ position at first, and the dislocation velocity is increased by hydrogen. At higher hydrogen concentration (Fig. 3b), the length of propagated atom columns become longer. At the 0.5$b$ position, some of the propagated columns combine with each other and the edge dislocation moves forward in a form similar to the classical kink-pair motion. But the structure here is not exactly a kink structure that always has a bowing-out shape with several Burgers vectors[7]. We will recall this structure as hydrogen induced broaden-core in the later discussions. The broaden-core always appears near the H atom positions which locally have low energy per atom, it suggests that the formation of this core structure is connected with the decrease of $E_{core}$.

The core structure of screw dislocation is illustrated using the differential displacement map (DDM), as shown in Fig. 4 where the small vectors indicate the relative [111] displacement of neighbouring Fe atoms. The easy-core configurations in Fig. 4a(I) and a(III) are typical non-polarized (or non-degenerate) cores[14], and the numbers in the figures represent the dislocation helicity located at each triangle[15]. The metastable configuration in Fig. 4a(II) contains two +1.0 easy-core structures separated by a hard-core triangle with −1.0 helicity, and this is the so-called split-core structure[15]. The existence of this core structure is still a debate[16] and we will discuss it later. The optimised hydrogen positions are located on the migration path of screw dislocation, and 0.7$b$ away from the initial dislocation position. In Fig. 4b(I), with hydrogen the helicity of triangle at easy-core position changes to +1.1. The displacement vectors near to the hydrogen atoms appear to be heterogeneous, which are related to the local strain field induced by hydrogen in different layers. When dislocation migrates to the 0.5$b$ position, an extra +0.8 core appears in the left of the easy-core position, which is different from the structure of split-core in Fig. 4a(II). Such screw core with hydrogen will be called as a quasi-split type in this report. As shown in Fig. 4b(III), the final configuration contains two easy-cores with +1.0 and +1.1 helicity separated by a −1.1 hard-core structure.

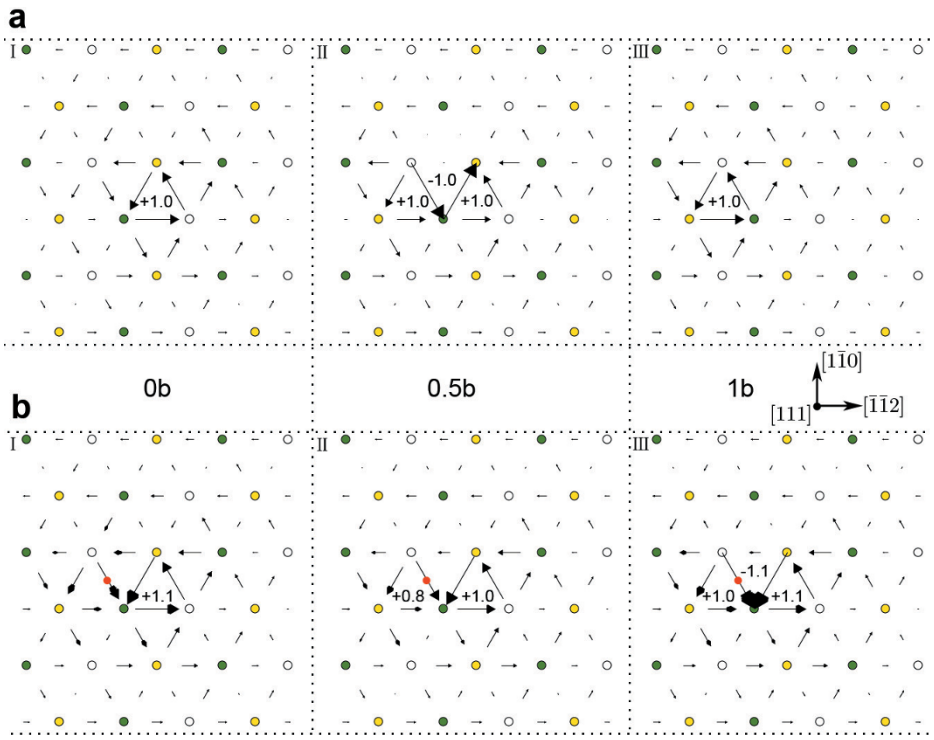


**Figure 4 | The differential displacement maps of screw dislocation with and without hydrogen.** Atomic positions are represented by three different colours to emphasise the fact that they belong to three different {111} layers: (a) hydrogen free; (b) at hydrogen concentration of 0.51 nm$^{-1}$, column of hydrogen atoms is marked with red dots.

## Discussion

Screw dislocation mobility enhanced by hydrogen should be emphasized here, because of high Peierls potential and the unrecoverable jogs it causes. Unlike the edge-H interaction, the shear modulus of screw-H system is unchanged, indicating that the change of core structure in short range is the main reason for the decreased Peierls potential. As illustrated before, this result is at variance with the guess from HELP theory, which is builded based on assuming isotropic strain field of H atoms.

The Peierls barrier of screw-H changes from camel-hump to single-hump shape. The shape of Peierls barrier is depending on whether the split-core (or hard-core) is metastable or not[15]. Pair and EAM potentials have evidenced the existence of camel-hump[17–19]. However, recently the DFT calculations on iron[15,16] ruled out the split-core structure as saddle point and support a single-hump. Despite the debate of saddle point, the EAM potentials and DFT simulations agree that screw dislocation migrates between two easy-core positions. According to our results, the final easy-core structure was changed to a quasi-split core by hydrogen. These core structures have potential energy only about 0.5 meV higher than the stable easy-core structure but much lower than the hydrogen free split-core. The single-hump obtained by the EAM potential is a consequence of this quasi-split core. The core structure evolutions of screw dislocation should take responsibility to the change of dislocation mobility and mechanical property for BCC metals. We note that the screw-H interaction is strongly depending on the hydrogen trapping position[4,7], investigation using different trap sites is needed in the future work.

In summary, we applied a DFT based embedded-atom method potentials to investigate the evolution of edge and crew dislocation core structures at different hydrogen concentrations. With hydrogen, the core energy and Peierls potential decrease as a function of hydrogen concentrations. The edge dislocation mobility is increased by the formation of a broaden-core structure. A quasi-split core structure is observed for screw dislocation with high hydrogen concentration. Because of the formation of such core structure, the screw Peierls barrier changes from camel-hump to single-hump type, it suggests that hydrogen influences the screw dislocation mobility not mainly due to the change of elastic constants, but the change of core structure.

## Methods

The MD simulations are performed using the LAMMPS code[20], with a DFT based Fe-H EAM potential reported by Ramasubramaniam et al[5]. Simulations are carried out by integrating Newton's equations of motion for all atoms using a time step of 1 fs. The optimization of structure was performed by the conjugate gradient (CG) algorithm, with a force tolerance of 0.001 eV/Å. The resulted lattice parameter $a$ for iron is 2.8553 Å. The Peierls barriers were investigated using the nudged elastic band (NEB) method, which enabled us to search the energy saddle-point and minimum energy path (MEP) between initial and final states. The initial configuration for NEB calculation was obtained by the isothermal-isobaric (NPT) ensemble with a Nose-Hoover thermostat, and the system was thermally equilibrated at 0.01 K for 50 ps. Then the canonical (NVT) ensemble was used instead and external stress $\tau_{xy}$ was applied on the surface atoms with a constant strain rate of $1.5 \times 10^7$ s$^{-1}$, as shown in Fig. 1. By the Peach-Koehler forces produced by $\tau_{xy}$, edge and screw dislocations move $1b$ forward along +X and −Z direction respectively, and these are the final configurations for NEB calculations. The dislocation displacement can be controlled by the average difference in displacement per atom between two $\{\bar{1}10\}$ surface, $\Delta u$. According to the Orowan's law, when $\Delta u = b$, the dislocation crosses the entire cell. Thus, for a displacement of $1b$, $\Delta u$ increases by $b/N_P$ with $N_P$ denotes the number of Peierls valleys along the moving direction.


1. Sofronis, P. & Birnbaum, H. K. Mechanics of the hydrogendashdislocationdashimpurity interactions—I. Increasing shear modulus. *J. Mech. Phys. Solids* **43**, 49–90 (1995).
2. Chateau, J. P., Delafosse, D. & Magnin, T. Numerical simulations of hydrogen-dislocation interactions in fcc stainless steels Part 1: hydrogen-dislocation interactions in bulk crystals. *Acta Mater.* **50**, 1507–1522 (2002).
3. Birnbaum, H. K. & Sofronis, P. Hydrogen-enhanced localized plasticity–a mechanism for hydrogen-related fracture. *Mater. Sci. Eng., A* **176**, 191–202 (1994).
4. Wang, S., Takahashi, K., Hashimoto, N., Isobe, S. & Ohnuki, S. Strain field of interstitial hydrogen atom in body-centered cubic iron and its effect on hydrogen–dislocation interaction. *Scripta Mater.* **68**, 249–252 (2013).
5. Ramasubramaniam, A., Itakura, M. & Carter, E. A. Interatomic potentials for hydrogen in α-iron based on density functional theory. *Phys. Rev. B* **79**, 174101 (2009).
6. Lee, B. J. & Jang, J. W. A modified embedded-atom method interatomic potential for the Fe–H system. *Acta Mater.* **55**, 6779–6788 (2007).
7. Wen, M., Fukuyama, S. & Yokogawa, K. Atomistic simulations of effect of hydrogen on kink-pair energetics of screw dislocations in bcc iron. *Acta Mater.* **51**, 1767–1773 (2003).
8. Cai, W., Li, J. & Yip, S. Molecular Dynamics. In Konings, R. J. M. (ed.) *Comprehensive Nuclear Materials*, 249–265 (Elsevier, Oxford, 2012).
9. Honeycutt, J. D. & Andersen, H. C. Molecular dynamics study of melting and freezing of small Lennard-Jones clusters. *J. Phys. Chem.* **91**, 4950–4963 (1987).
10. Hirth, J. P. & Lothe, J. *Theory of Dislocations* (John Wiley & Sons, New York, 1982), 2ed edn.
11. Mendelev, M. I. *et al*. Development of new interatomic potentials appropriate for crystalline and liquid iron. *Philos. Mag.* **83**, 3977–3994 (2003).
12. Domain, C. & Monnet, G. Simulation of screw dislocation motion in iron by molecular dynamics simulations. *Phys. Rev. Lett.* **95**, 215506 (2005).
13. Chasussidon, J., Fivel, M. & Rodney, D. The glide of screw dislocations in bcc Fe: Atomistic static and dynamic simulations. *Acta Mater.* **54**, 3407–3416 (2006).
14. Takeuchi, S. Core structure of a screw dislocation in the b.c.c. lattice and its relation to slip behaviour of α-iron. *Philos. Mag.* **39**, 661–671 (1979).
15. Itakura, M., Kaburaki, H. & Yamaguchi, M. First-principles study on the mobility of screw dislocations in bcc iron. *Acta Mater.* **60**, 3698–3710 (2012).
16. Ventelon, L. & Willaime, F. Core structure and Peierls potential of screw dislocations in - Fe from first principles: cluster versus dipole approaches. *J. Comput. Aided Mater. Des.* **14**, 85–94 (2008).
17. Gordon, P. A., Neeraj, T., Li, Y. & Li, J. Screw dislocation mobility in BCC metals: the role of the compact core on double-kink nucleation. *Modell. Simul. Mater. Sci. Eng.* **18**, 085008 (2010).
18. Gilbert, M. R. & Dudarev, S. L. Ab initiomulti-string Frenkel–Kontorova model for a b = a/2[111] screw dislocation in bcc iron. *Philos. Mag.* **90**, 1035–1061 (2010).
19. Edagawa, K., Suzuki, T. & Takeuchi, S. Motion of a screw dislocation in a two-dimensional Peierls potential. *Phy. Rev. B* **55**, 6180–6187 (1997).
20. Plimpton, S. Fast parallel algorithms for short-range molecular dynamics. *J. Comput. Phys.* **117**, 1–19 (1995).


## Acknowledgements

This work was conducted at Hokkaido University, supported by "Nanotechnology Platform" Program of the MEXT, Japan. A part of this work is suppoted by Hokkaido university academic cloud, information initiative center.

## Author contributions

S.W. wrote the main manuscript text, N.H. and S.O. supervised this work. All authors reviewed the manuscript.

## Additional information

**Competing financial interests:** The authors declare no competing financial interests.

**How to cite this article:** Wang, S., Hashimoto, N. & Ohnuki, S. Hydrogen-induced change in core structures of {110}[111] edge and {110}[111] screw dislocations in iron. *Sci. Rep.* **3**, 2760; DOI:10.1038/srep02760 (2013).